Electronic Supplementary Information for:

A luminescent MOF based on pyrimidine-4,6-dicarboxylate ligand and lead(II) with unprecedented topology

Laura Razquin-Bobillo †, [1] Oier Pajuelo-Corral †, [1] Andoni Zabala-Lekuona, [1] Iñigo Vitorica-Yrezabal, [2] Jose Angel García, [3] Jose M. Moreno, [2] Antonio Rodríguez-Diéguez [2] and Javier Cepeda [1,*]

1 Departamento de Química Aplicada, Facultad de Química, Universidad del País Vasco/Euskal Herriko Unibertsitatea (UPV/EHU), 20018, Donostia, Spain.

2 Departamento de Química Inorgánica, Facultad de Ciencias, Universidad de Granada, 18071, Granada, Spain.

3 Departamento de Física, Facultad de Ciencia y Tecnología, Universidad del País Vasco/Euskal Herriko Unibertsitatea (UPV/EHU), 48940, Leioa, Spain.

† These authors contributed equally to this work.

Contents:

S1. Additional structural details.

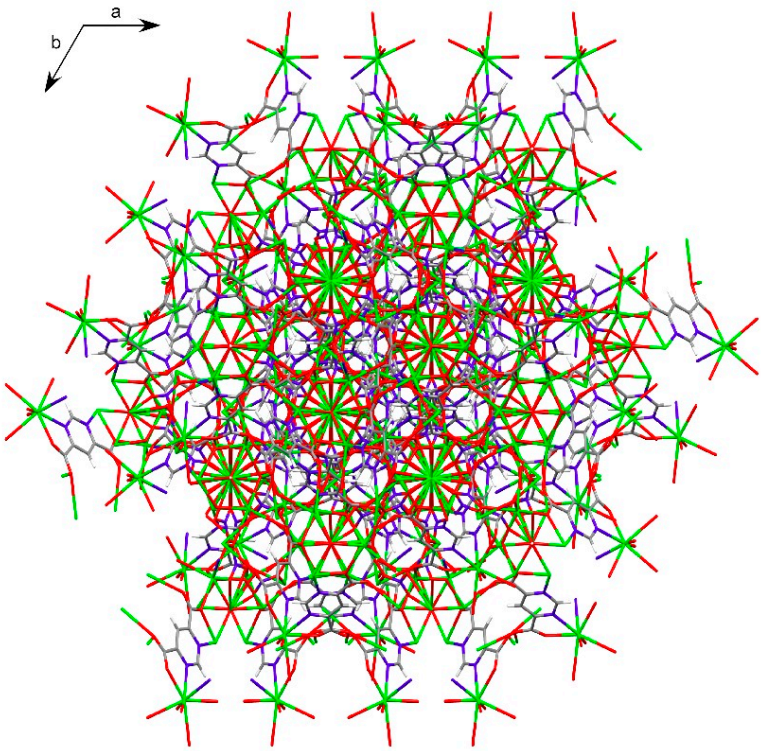

Figure S1. Packing of compound **1** along the *c* axis viewing direction.

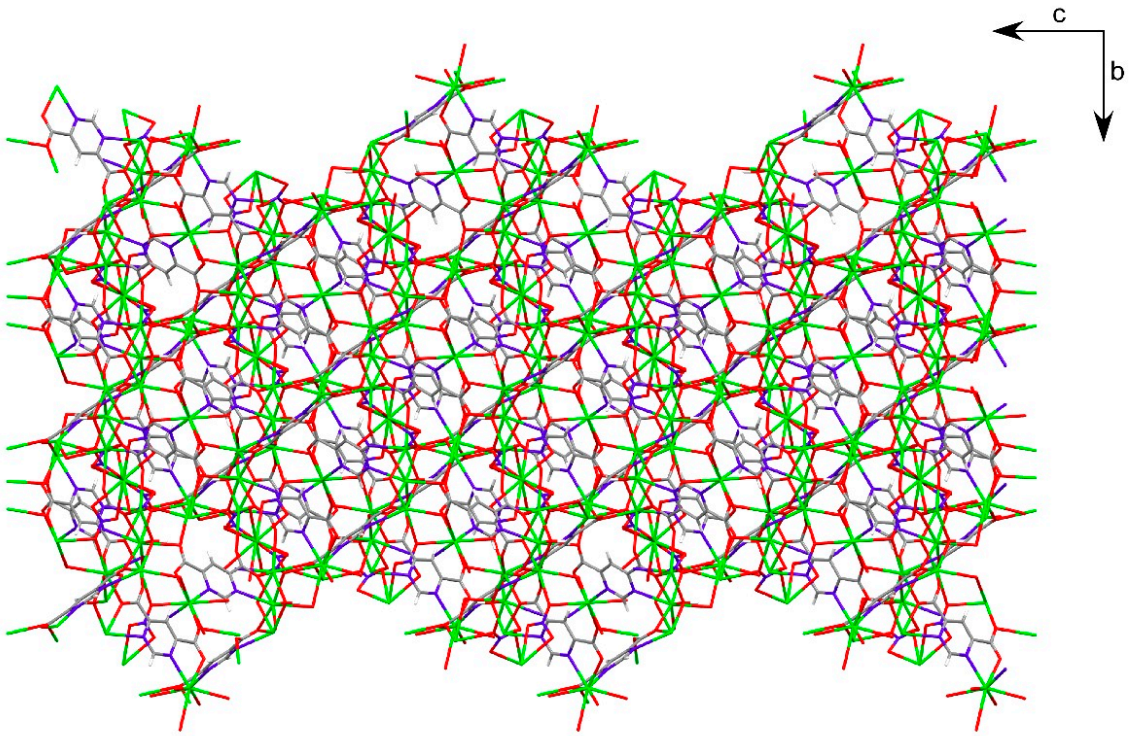

Figure S2. Packing of compound **1** along the *a* axis viewing direction.

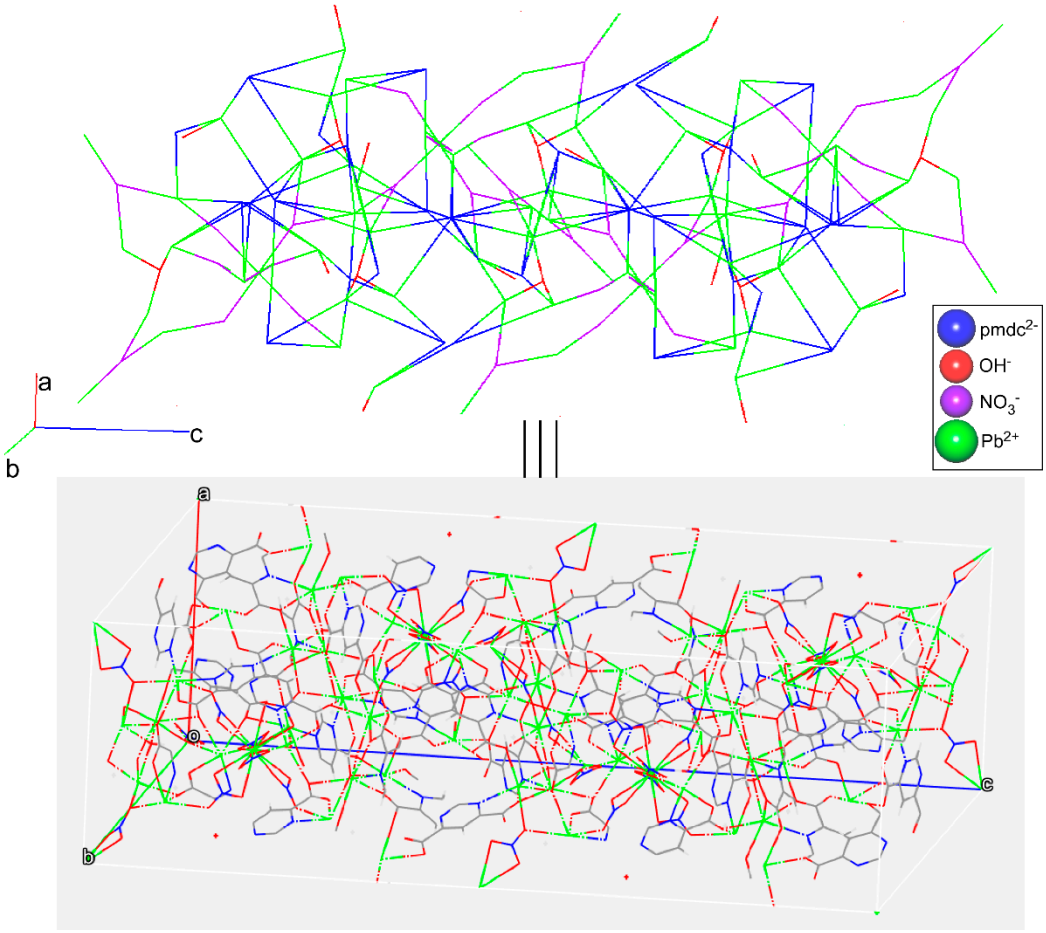

Figure S3. Crystal packing of compound **1** drawn in the form of topological network (top) and molecular framework (bottom).

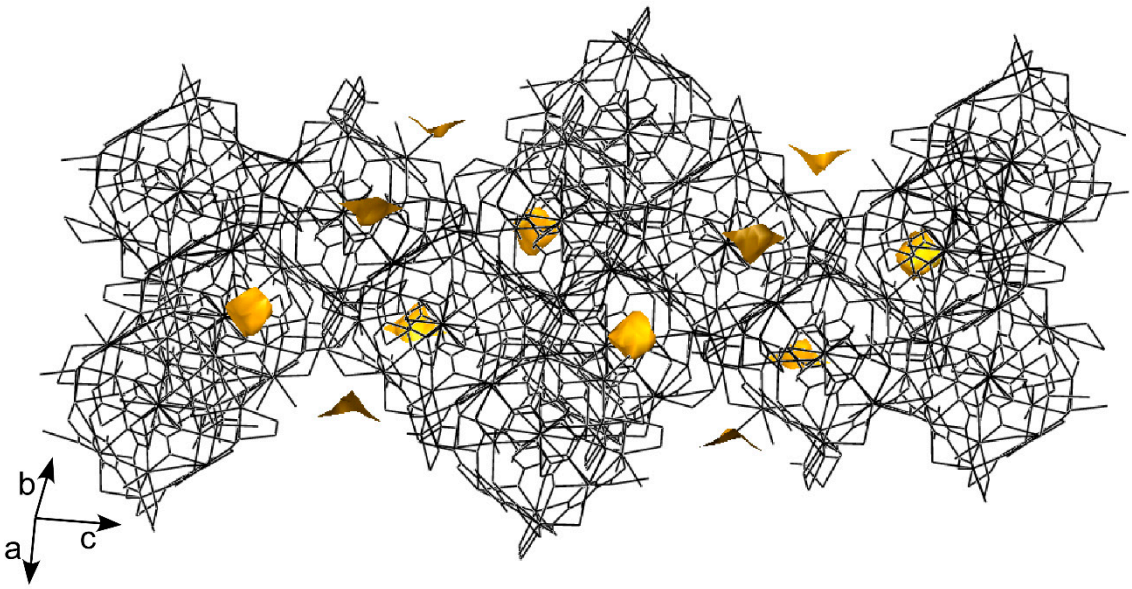

Figure S4. Crystal packing of compound **1** showing the isolated voids (golden solid) containing water molecules.

S2. Continuous Shape Measurements (CShMs).

Table S1. Continuous shape measurements for the coordination environments for compound **1**. The lowest SHAPE values are shown in bold blue, indicating best fits.

Codes:

HP-7 1 D_{7h} Heptagon

HPY-7 2 C_{6v} Hexagonal pyramid

PBPY-7 3 D_{5h} Pentagonal bipyramid

COC-7 4 C_{3v} Capped octahedron

CTPR-7 5 C_{2v} Capped trigonal prism

JPBPY-7 6 D_{5h} Johnson pentagonal bipyramid J13

JETPY-7 7 C_{3v} Johnson elongated triangular pyramid J7

Structure [ML7]	HP-7	HPY-7	PBPY-7	COC-7	CTPR-7	JPBPY-7	JETPY-7
Pb1	32.503	19.509	5.861	2.872	**2.159**	9.258	20.855

Codes:

OP-8 1 D_{8h} Octagon

HPY-8 2 C_{7v} Heptagonal pyramid

HBPY-8 3 D_{6h} Hexagonal bipyramid

CU-8 4 O_h Cube

SAPR-8 5 D_{4d} Square antiprism

TDD-8 6 D_{2d} Triangular dodecahedron

JGBF-8 7 D_{2d} Johnson gyrobifastigium J26

JETBPY-8 8 D_{3h} Johnson elongated triangular bipyramid J14

JBTPR-8 9 C_{2v} Biaugmented trigonal prism J50

BTPR-8 10 C_{2v} Biaugmented trigonal prism

JSD-8 11 D_{2d} Snub diphenoid J84

TT-8 12 T_d Triakis tetrahedron

ETBPY-8 13 D_{3h} Elongated trigonal bipyramid

Structure [ML8]	OP-8	HPY-8	HBPY-8	CU-8	SAPR-8	TDD-8	JGBF-8
Pb2	27.041	24.070	16.303	10.258	**1.768**	3.401	13.684

Structure [ML8]	JETBPY-8	JBTPR-8	BTPR-8	JSD-8	TT-8	ETBPY-8
Pb2	24.012	3.876	3.624	5.445	10.587	19.375

Codes:

DP-12	1 D_{12h}	Dodecagon
HPY-12	2 C_{11v}	Hendecagonal pyramid
DBPY-12	3 D_{10h}	Decagonal bipyramid
HPR-12	4 D_{6h}	Hexagonal prism
HAPR-12	5 D_{6d}	Hexagonal antiprism
TT-12	6 T_d	Truncated tetrahedron
COC-12	7 O_h	Cuboctahedron
ACOC-12	8 D_{3h}	Anticuboctahedron J27
IC-12	9 I_h	Icosahedron
JSC-12	10 C_{4v}	Johnson square cupola J4
JEPBPY-12	11 D_{6h}	Johnson elongated pentagonal bipyramid J16
JBAPPR-12	12 C_{2v}	Biaugmented pentagonal prism J53
JSPMC-12	13 C_s	Sphenomegacorona J88

Structure [ML12]	DP-12	HPY-12	DBPY-12	HPR-12	HAPR-12	TT-12	COC-12
Pb3	31.836	28.687	19.525	10.661	17.152	11.788	**1.830**

Structure [ML12]	ACOC-12	IC-12	JSC-12	JEPBPY-12	JBAPPR-12	JSPMC-12
Pb3	7.325	5.604	20.646	11.573	12.422	19.913

S3. Powder X-ray Diffraction Analysis.

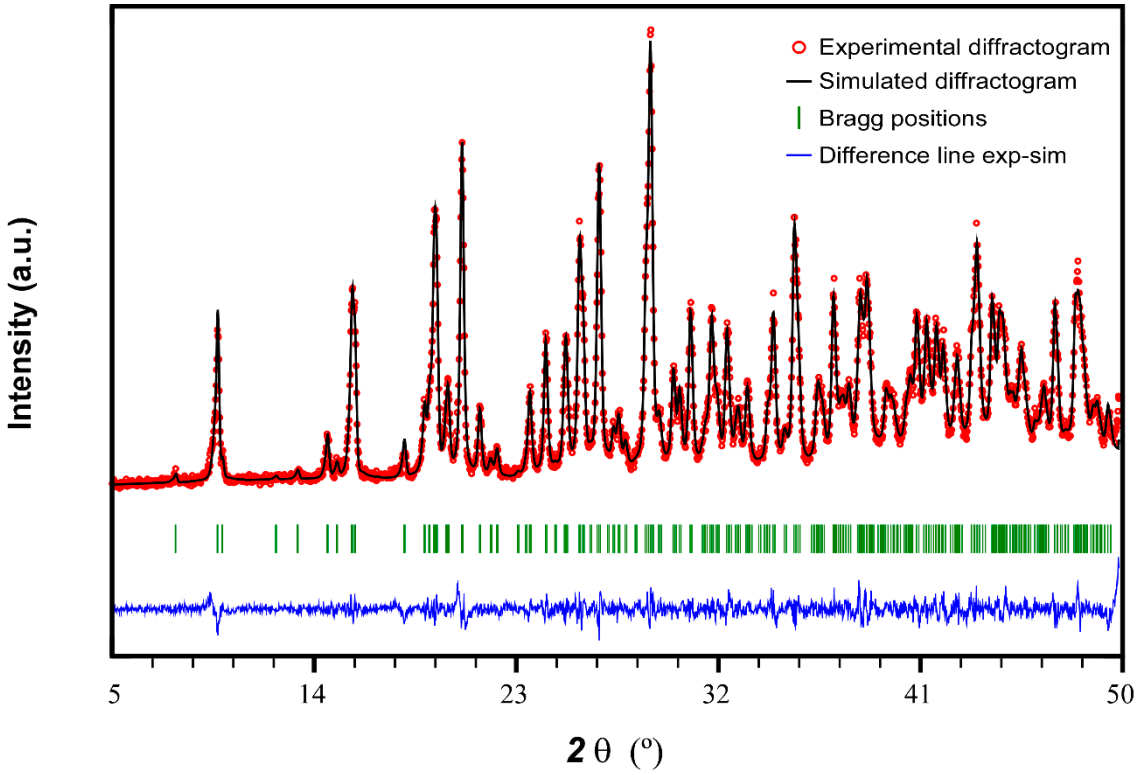

Figure S5. Pattern-matching analysis of polycrystalline sample of compound **1**.

S4. FT-IR spectroscopy.

Infrared spectroscopy was used as an initial characterization technique to check the presence of pmdc in compound **1** (Figure S4). Table S2 shows the wavenumbers of the most relevant bands, together with their relative intensities and the proposed assignation in each case for compound **1**.

The spectrum of compound **1** shows a broad and intense band in the frequency region of 3550-3100 cm^{-1}, assigned to the characteristic peaks of the OH vibration of free water molecules and to the C-H vibration of the pyrimidinic ring of the pmdc ligand. The intense vibrations around 1650 cm^{-1} and 1360 cm^{-1} correspond to the asymmetric and symmetric stretching vibrations of the carboxylate groups. At 1385 cm^{-1} the strong vibration of the nitrate anion appears, while in the 1300-1000 cm^{-1} region several medium- and weak-intensity peaks appear that can be attributed to the distortions originated in the aromatic ring of pmdc ligand. The vibration bands of the M-O and M-N bonds are observed below 550 cm^{-1}.

Table S2. Main IR absorption bands (cm^{-1}) for compound **1**.[a]

Asig.[b]	Compound **1**
ν (O–H)	3470m, 3170m
ν (C–H)	3075m
ν_{as}(O–C–O) + ν (C=C + C=N)	1635s, 1600s, 1585sh, 1535s
ν (C_{ar}–C)	1460w
ν_s (O–C–O)	1360s, 1305w
ν (NO_3)	1385s
δ_{ip}(C–H)	1285m, 1185m, 1095w, 1040w, 1015m
δ_{op}(C–H)	940w
δ_{ring}	835m
δ_{ip}(O–C–O)	810m
δ_{op}(O–C–O)	730s, 715ss
τ_{ring}	695m, 670m, 560w
ν (M–O + M–N)	505w, 485w, 445w, 415w

[a] vs: very strong, s: strong, m: medium, w: weak, and sh: shoulder. [b] ν: stretching, δ: bending, ip: inside plane, op: out of plane, s: symmetric, and as: antisymmetric.

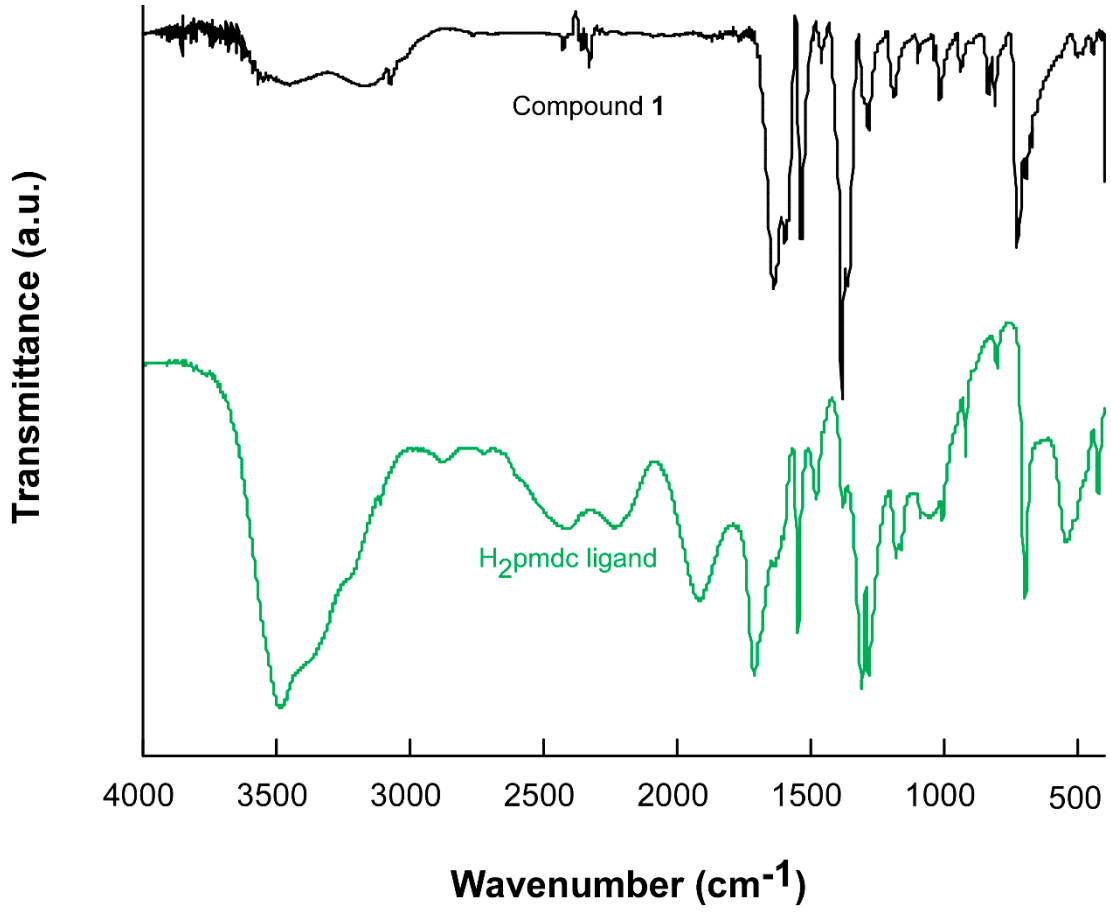

Figure S6. Comparison of the FTIR spectra of compound **1** and the free H_2pmdc ligand.

S5. Photoluminescence measurements and calculations.

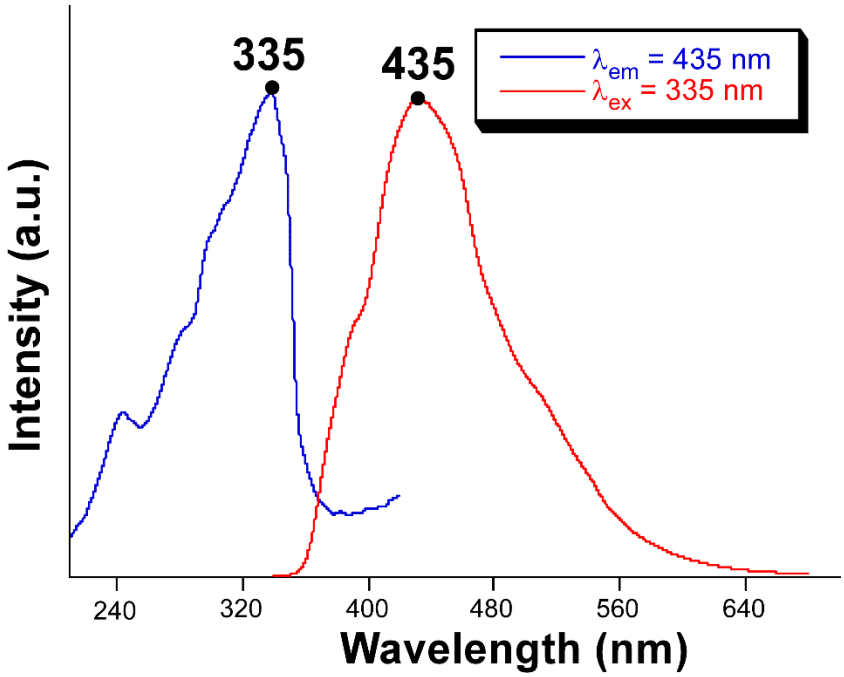

Figure S7. Excitation (λ_{em} = 435 nm) and emission (λ_{ex} = 335 nm) spectra of the H2pmdc ligand recorded at room temperature.

The emission lifetimes were estimated by measuring the decay curves for both maxima. The signal for the first maximum was so weak and the lifetime quite short so it was estimated by deconvolution. On the contrary, the lifetime of the maximum at 550 nm was estimated by a tail fitting procedure and gave a component of 5.71(59) μs with a weight of 40% and a second component of 116.4(34) μs with a weight of 60%.

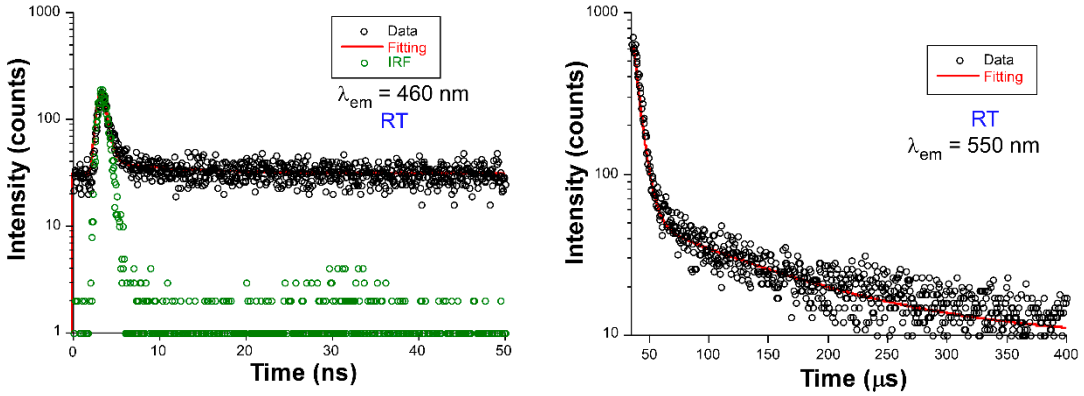

Figure S8. Decay curves of the emission of compound **1** at room temperature for the main emission maxima.

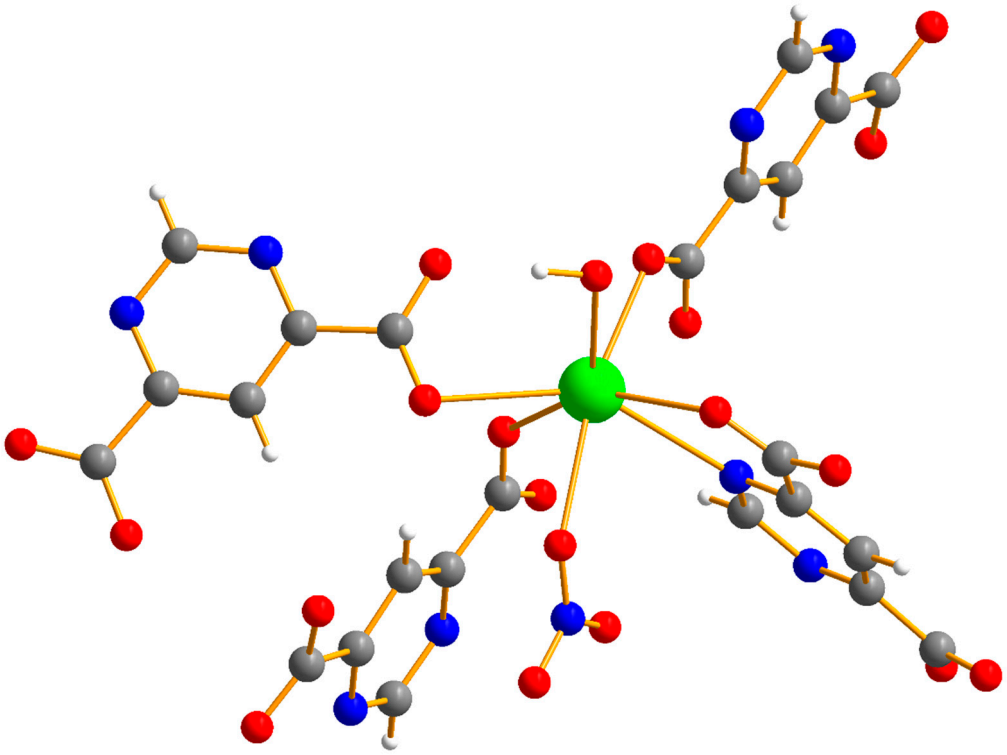

Figure S9. Monomeric model taken from the X-ray coordinates used for the calculations of the PL properties of compound **1**.

Table S3. Calculated main excitation and emission energies (nm), singlet electronic transitions, and associated oscillator strengths of a model of compound **1** in gas phase.

Exc. state	Calcd. λ (nm)	Significant contributions	Osc. strength (a.u.)
		Excitation energies	
7	395	HOMO – 5 → LUMO (99%)	0.1421
10	335	HOMO – 7 → LUMO (99%)	0.0356

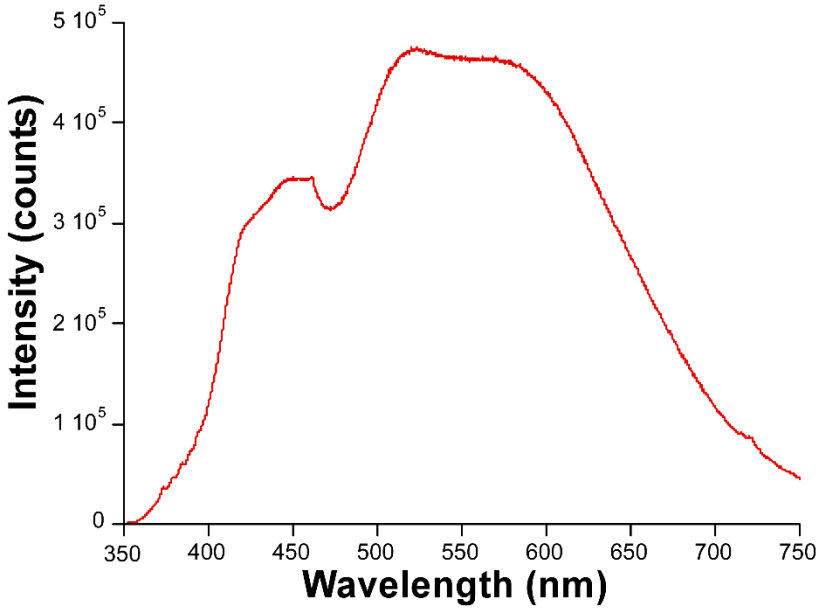

Figure S10. Emission spectrum of compound **1** collected at 15 K under monochromatic laser light (λ_{ex} = 325 nm).

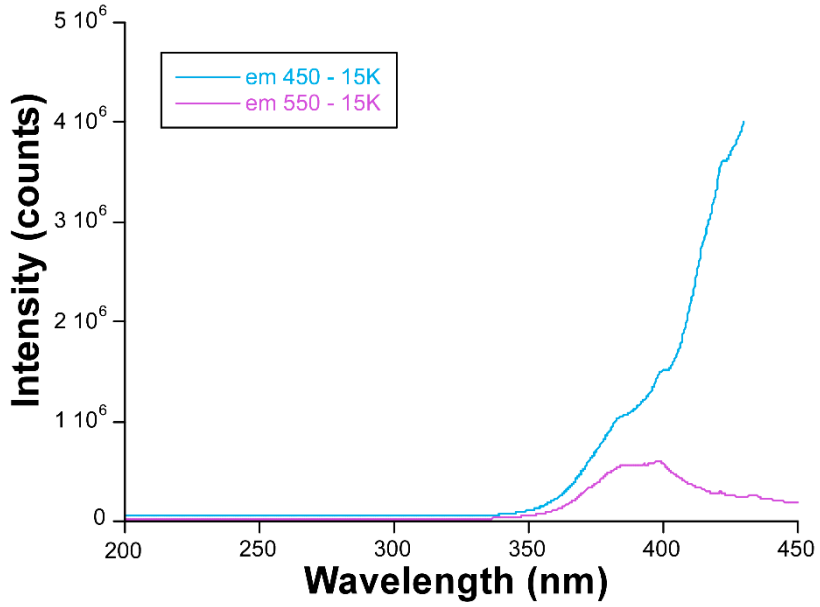

Figure S11. Comparison of the low temperature excitation spectra collected over the two maxima observed in the emission of compound **1**.

The emission lifetimes for the low temperature decay curves were estimated with the same fitting procedure explained for RT measurements by measuring the decay curves for both maxima. The signal for the first maximum was so weak and the lifetime quite short so it was estimated by deconvolution. On the contrary, the lifetime of the maximum at 550 nm was estimated by a tail fitting procedure and gave a component of 5.71(59) μs with a weight of 40% and a second component of 116.4(34) μs with a weight of 60%.

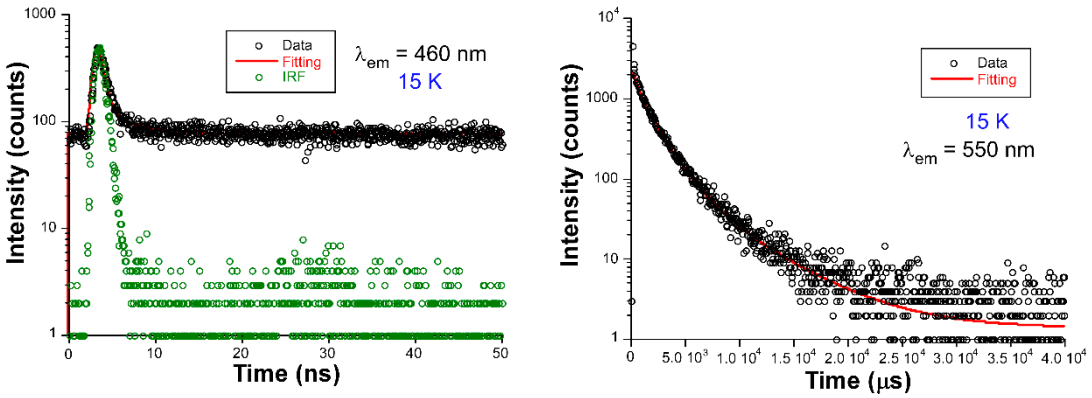

Figure S12. Decay curves of the emission of compound **1** at low temperature for the main emission maxima.

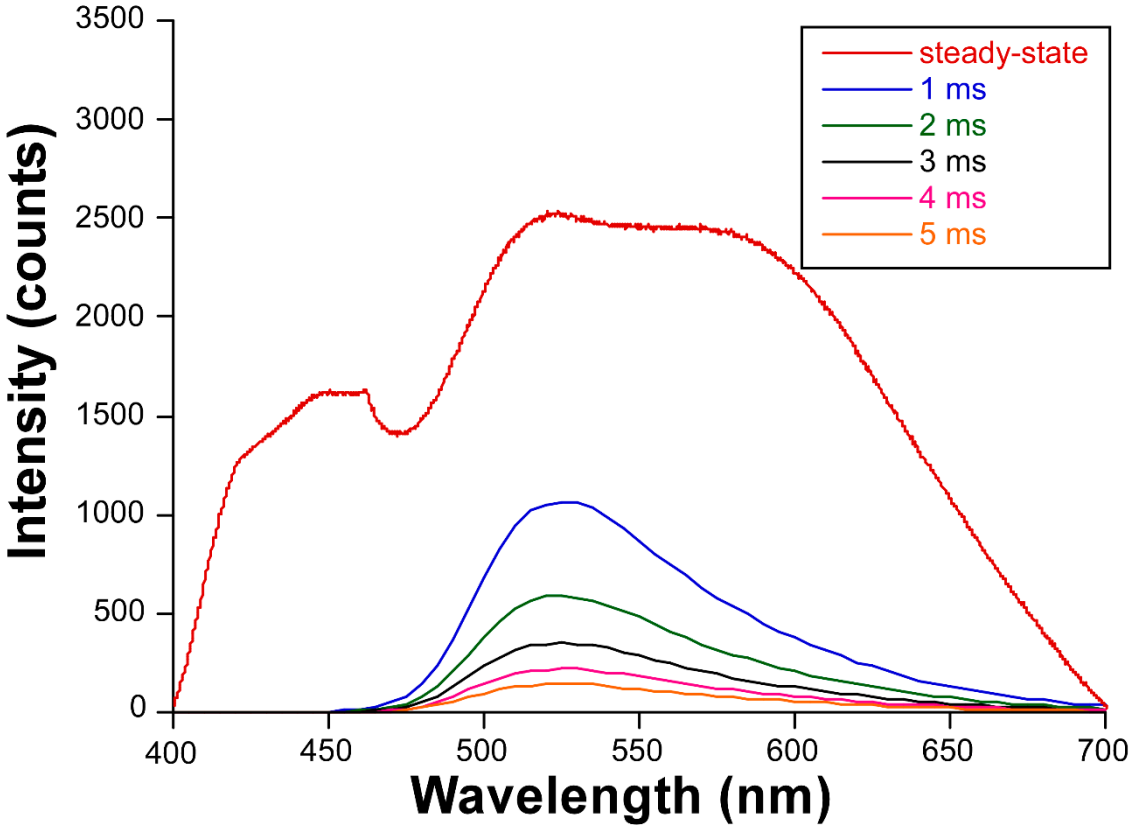

Figure S13. TRES recorded at 15 K for compound **1** showing a selection of spectra.

S6. Diffuse reflectance.

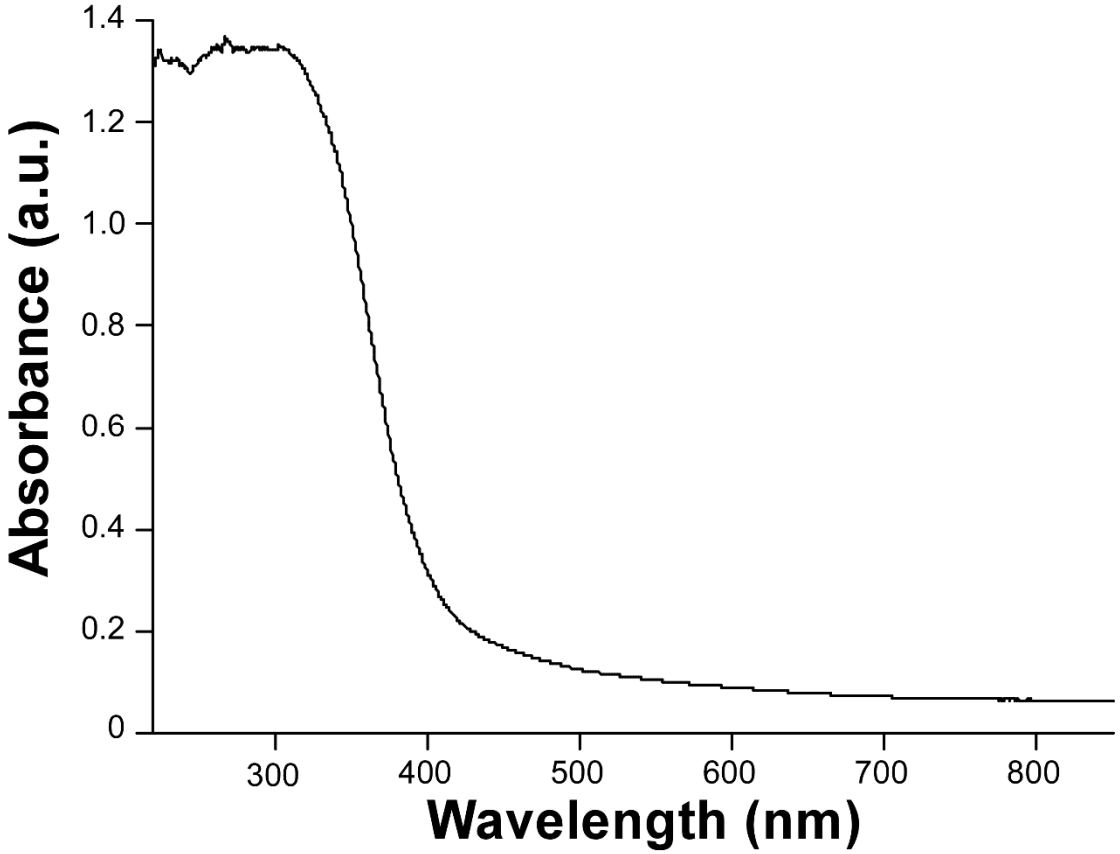

Figure S14. Diffuse reflectance spectrum acquired on a polycrystalline sample of compound **1**.